EEG-based neurofeedback with network components extraction: data-driven approach by multilayer ICA extension and simultaneous EEG-fMRI measurements

Takeshi Ogawa[1*], Hiroki Moriya[1], Nobuo Hiroe[2], Motoaki Kawanabe[1,3], Jun-ichiro Hirayama[3,4]

[1]Cognitive Mechanisms Laboratories, Advanced Telecommunications Research Institute International, Seika-Cho, Soraku-gun, Kyoto, Japan

[2]Neural Information Analysis Laboratories, Advanced Telecommunications Research Institute International, Seika-Cho, Soraku-gun, Kyoto, Japan

[3]RIKEN Center for Advanced Intelligence Project, Seika-Cho, Soraku-gun, Kyoto, Japan

[4]Human Informatics and Interaction Research Institute, National Institute of Advanced Industrial Science and Technology (AIST), Tsukuba City, Ibaraki, Japan

*Correspondence:

Takeshi Ogawa, Ph.D

t.ogawa@atr.jp

Abstract

Several studies have reported that advanced treatments for depressive symptoms, such as a real-time functional MRI (fMRI) neurofeedback, have been reported. The fMRI neurofeedback focusing on a regularization of functional connectivity (FC) between executive control network (ECN) and default mode network (DMN) has been achieved to support the reduction of depressive symptoms. However, it is difficult to install this system anywhere and repetitively provide the treatment in practice because the cost is high. Additionally, no practical signal processing techniques have existed so far to extract FC-related features from electroencephalography (EEG) signals, particularly when no physical forward models are available. In this regard, stacked pooling and linear components estimation, recently proposed as a multilayer extension of independent component analysis (ICA) and related independent subspace analysis (ISA), can be a promising alternative. However, its application to the resting-state EEG has never been investigated so far. We expected that if the extracted EEG network features were correlated with fMRI network activity corresponding to DMN or ECN, it might help modulate the target FC in the EEG-based neurofeedback training.

Here, we developed a real-time EEG neurofeedback system for improving depressive symptoms by using an EEG network features estimated by SPLICE. Utilizing information of the fMRI biomarker, we examined our paradigm for upregulation of the dorsolateral prefrontal cortex (DLPFC)/middle frontal cortex or downregulation of precuneus/posterior cingulate cortex (PCC). We conducted a three-day NF experiment for the neurofeedback group (n=8; NF group) and sham group (n=9). To this end, we found a large effect size in the rumination response scale score (total, brooding, and reflection) in the comparison between NF and sham groups. Additionally, brain signals of the tasked fMRI (a contrast

of 2-back > 0-back) in the neurofeedback group were significantly decreased in the right cuneus and DLPFC compared to the control group. We demonstrated possibilities of EEG neurofeedback treatment for depressive symptoms using EEG network features extracted by SPLICE in the subclinical trials.

Keywords: neurofeedback, depression, EEG-fMRI, blind source separation, functional connectivity

1. Introduction

Advanced treatments for depressive symptoms have been studied using brain or physiological measurement instead of traditional medical treatments. One of the noninvasive ways to accurately monitor brain activity that may represent depressive symptoms is functional MRI (fMRI) because of its high spatial resolution, even around deep brain areas. Recently, several groups have proposed real-time fMRI neurofeedback paradigms that participants could regulate their brain signals from states/conditions of depressive symptoms to healthy ones (Young et al., 2017; Yamada et al., 2017; Taylor et al., 2021). During the intervention of the real-time neurofeedback, participants can control their brain activity to be closed to the healthy condition and then reduce their depressive symptoms.

By using the real-time fMRI neurofeedback, several studies have reported efficacies for depressive symptoms. However, it is difficult to install this system anywhere and repetitively provide the treatment in practice because of the expensive costs. On the other hand, the real-time neurofeedback using electroencephalography (EEG) has been proposed as an alternative approach, e. g., frontal alpha asymmetry (Wang et al., 2019), peak alpha frequency (Yu et al., 2020), and alpha-theta ratio (Cheon et al., 2016). In particular, the frontal alpha asymmetry EEG neurofeedback has been examined to modulate left-side alpha power associated with brain activity in the left amygdala. EEG has many practical benefits, such as reasonable cost, high-temporal resolution, and low physical constraints, while a low-spatial resolution is detrimental. Recent studies of EEG-fMRI data have reported possibilities of the effectiveness of real-time neurofeedback for depression (Zotev et al., 2014; Zotev et al., 2016; Zotev et al., 2020) and improved the

reliability of EEG signature for neurofeedback. In these neurofeedback training (NF training), participants are asked to imagine their positive autographic memory, such as happy events, and to increase brain activity in the left amygdala and frontal alpha asymmetry at the same time. Thus, this neurofeedback aims to regulate their brain functions in the left amygdala, similar to the healthy state.

Another recent approach has also been developed for fMRI neurofeedback focusing on regularizing functional connectivity (FC) between executive control network (ECN) and default mode network (DMN) for depression (Yamada et al., 2017; Taylor et al., 2021; Tsuchiyagaito et al., 2020). A relationship of time courses between ECN and DMN in healthy individuals is generally anticorrelated, and it is associated with the distinction between internal (e.g., own thoughts) and external (e.g., perceptions of the external environment) contents (Northoff, 2016). In contrast to healthy individuals, the case of depressive disorder tends to be dysbalanced. Then it increases self-focus (rumination, guilt, fear) and decreases environment-focus (social withdrawal, psychomotor retardation) (Drysdale et al., 2017). This relationship is elucidated in the fMRI biomarker, which was identified FCs to classify patients with melancholic depression and healthy controls utilizing data-driven approaches (Ichikawa et al., 2020; Yamashita et al., 2020). Especially, FC between the dorsolateral prefrontal cortex (DLPFC)/middle frontal gyrus (MFG) in ECN and the precuneus/posterior cingulate cortex (PCC) in DMN was shown to be necessary. According to the results of the fMRI biomarker, neurofeedback with particular FC, called FC neurofeedback (FCNef), is expected a new type of treatment for depression with precise localization.

However, in contrast to the real-time fMRI feedback or FCNef, an EEG neurofeedback using network features has been poorly investigated. The reason is mainly that no practical signal processing techniques have existed so far to extract FC-related features from EEG signals, particularly when no physical forward models are available. In fact, most studies have used sensor-level features such as time-instant powers of particular frequency bands or sought to extract source-level features by a blind-source separation (BSS) technique such as independent component analysis (ICA). Neither method is not designed to detect EEG features that reflect FC and modular organization related to the resting-state networks. Therefore, a new BSS-based technique is strongly required, combined with a signal model that explicitly assumes network structures at the source level related to the FC. In this regard, stacked pooling and linear components estimation (SPLICE; Hirayama et al., 2017), recently proposed as a multilayer extension of ICA and related independent subspace analysis (ISA; Hyvärinen & Hoyer, 2000), can be a promising alternative, although its application to the resting-state EEG has never been investigated so far. We expected that if the extracted EEG network features correlated with fMRI network activity corresponding to DMN or ECN, it might help modulate the target FC in the EEG-based NF training.

Here, we have attempted to extend an EEG network estimated by SPLICE for a real-time EEG NF paradigm. We have developed EEG-based NF training to improve depressive symptoms for healthy individuals who tended to depression. We examined EEG-NF to modulate estimated brain activity, the DLPFC/MFC as upregulation or precuneus/PCC as downregulation, then decrease depressive symptoms. We conducted a three-day EEG-NF paradigm with two groups (neurofeedback: NF; sham)

of subclinical participants with depressive symptoms targeting regions (DLPFC/MFC or precuneus/PCC) while referring to an FCNef paradigm (Yamada et al., 2017; Taylor et al., 2021). For training of the SPLICE model, participants completed two-day EEG-fMRI experiments to acquire EEG-fMRI simultaneous recorded data at resting and during N-back tasks. By modeling SPLICE from the resting-state data of EEG-fMRI, we selected EEG network features correlated with fMRI signals in the DLPFC/MFG or precuneus/PCC for NF training. Scores on the Beck Depression Inventory-II (BDI-II; Beck et al., 1996) and the Rumination Response Scale (RRS; Hasegawa, 2013) were measured pre-and post-NF training. Finally, we evaluated the effect size of the difference between pre-and post-NF among neurofeedback and sham groups, then described a possibility of EEG-neurofeedback using EEG network features relevant to fMRI network information.

2 Materials and Methods

2.1 SPLICE

SPLICE (Hirayama et al., 2017) is a multilayer extension of ICA based on a probabilistic model that simplifies the generative process of EEG. Let $\mathbf{x}$ and $\mathbf{s}$ denote the vectors of EEG measurements and unobserved source signals, respectively, at a single time point. Then, we assume a linear model (first layer) similar to ICA, given by

$$\mathbf{x} = \mathbf{A}\mathbf{s}, \tag{1}$$

where mixing matrix $\mathbf{A}$ is square and invertible; the inverse $\mathbf{W} := \mathbf{A}^{-1}$ is called demixing matrix. Both $\mathbf{x}$ and $\mathbf{s}$ are zero-mean, without loss of generality, by subtracting the sample mean in advance from original data vectors. Note that the sources (i.e., entries in $\mathbf{s}$) lack explicit physical mapping to the cortex. However, they can still be interpretable as

reflecting cortical activations based on their associated topographies (i.e., corresponding columns of $\mathbf{A}$), exactly the same case as ICA. For mathematical convenience, the number of sources, d, is assumed to be the same as the dimensionality of $\mathbf{x}$; in practice, we apply PCA beforehand to determine an appropriate number of sources as customarily done in ICA.

On top of the first linear layer, the additional layers are introduced to model statistical dependency among the sources and parametric structures behind it. Specifically, SPLICE introduces 1) functional modularity of sources and 2) intrinsic correlations (coactivations) among modules into the multilayer generative model. Both are reasonable assumptions in particular for the resting-state EEG data because cortical activity at rest is known to exhibit functional organization with multiple modules (e.g., resting-state network), often mutually correlated or anticorrelated.

Formally, we divide the d first-layer sources into m modules $\mathbf{s}_{[j]}$ without overlapping, where $\mathbf{s}_{[j]}$ denotes the vector consisting of d_j sources belonging to module j ($d = \sum_{j=1}^{m} d_j$). $\mathbf{s}_{[j]}$ represents a d_j-dimensional subspace spanned by the corresponding columns in $\mathbf{A}$. Then, we assume that modules $\mathbf{s}_{[j]}$ have mutually correlated (squared) L2-norms $||\mathbf{s}_{[j]}||^2$, generated by an additional ICA-like linear model with pointwise nonlinearity, such that

$$||\mathbf{s}_{[j]}||^2 = \boldsymbol{F}_j^{-1}\left([\mathbf{A}'\mathbf{s}']_j\right), j = 1, 2, \ldots, m, \qquad (2)$$

Where an appropriate link function $\boldsymbol{F}_j$ is used for a convention between nonnegative (norm) and real random variables (we set $\boldsymbol{F}_j$ = log in our analysis); $\mathbf{A}'$ and $\mathbf{s}'$ are invertible mixing matrix and source vector (and $\mathbf{W}' := \mathbf{A}'^{-1}$ is a demixing matrix) of this layer, and $[\cdot]_j$ denotes the j-th entry of a vector. Given the norms, every $\mathbf{s}_{[j]}/||\mathbf{s}_{[j]}||$ is assumed to be

uniformly distributed on a unit hypersphere, independently of any other random variables, making the model non-informative except for the distribution of the norms. Note that the model can actually be recursively extended to have additional layers to further model the dependency in higher-layer sources (Hirayama et al., 2017). However, in the present study, we simply assume Eq.(2) to be the top layer. The entries in $\mathbf{s}'$ are thus assumed to be independent of each other, given a typical prior in ICA (e.g., the one corresponding to the standard $tanh$ nonlinearity).

To recapitulate the model, we illustrate a conceptual diagram of SPLICE in Figure 1. The model consists of three layers, two linear layers, and an intermediate L2-pooling layer calculating the norms. Here, we define $\mathbf{x}' := \mathbf{A}'\mathbf{s}'$. If the highest layer $\mathbf{A}'$ is not diagonal, modules are mutually independent, and the model, in fact, reduces to that of independent subspace analysis (Hyvärinen & Hoyer, 2000). If not diagonal, the modules are not independent and thus expected to be suitable to represent correlated or anticorrelated cortical modules. Note that modeling non-diagonal $\mathbf{A}'$ not only affects the higher layer but also influences the first layer through the joint learning of the two layers (see below) because it makes a different (possibly improved) prior assumption on the first layer sources that of ICA or ISA.

A striking property of SPLICE is that both parameter estimation (learning) and posterior inference on latent variables can be performed in a principled manner without resorting to any approximative techniques or heavy numerical computation. Learning is done based on conventional maximum likelihood (ML) estimation. The corresponding loss function, i.e., negative log-likelihood for a single datum $\mathrm{L} := -\ln p(\mathbf{x}) + \mathrm{const.}$, is analytically

given by

$$L = \sum_{k=1}^{m} \boldsymbol{H}_k \left(\sum_{k=1}^{m} w'_{kj} \boldsymbol{F}_j \left(\left\| \mathbf{W}_{[j]} \mathbf{x} \right\|^2 \right) \right) - \ln|det\mathbf{W}'| + \sum_{k=1}^{m} \boldsymbol{G}_j \left(\left\| \mathbf{W}_{[j]} \mathbf{x} \right\|^2 \right) - c \ln|det\mathbf{W}| \quad (3)$$

where $\boldsymbol{H}$ and $\boldsymbol{G}$ are functions derived from the prior distribution on $\mathbf{s}$' and link function $\boldsymbol{F}_j$. The dimensionality of every module (subspace) d_j is adaptively determined before the ML estimation using a clustering-like technique (see Hirayama et al., 2017 for details).

Once demixing matrices $\mathbf{W}$ and $\mathbf{W}$' are learned, one can readily invert the generative process by computing $\mathbf{s} = \mathbf{W}\mathbf{x}$ and $\mathbf{s}' = \mathbf{W}'\mathbf{x}'$, with the L2-pooling $||\mathbf{s}_{[j]}||^2$ (followed by $\boldsymbol{F}_j$) between them. In practice, the pooled outputs (squared norm) may fluctuate too heavily due to the noisy nature of EEG. Thus, as a slight extension of the original SPLICE, we also implemented the L2-pooling across successive time points for smoothing, which was done in a principled manner by modifying the model and likelihood, so that the top linear layer determines the L2 norm of $\mathbf{s}_{[j]}$ that now concatenates several instances of the d_j sources across time points. Note that the pooling just means taking the sum of squares (of the filtered outputs). Thus, the squared module norm essentially gives the total power or energy of a source module's activity. We, therefore, focused primarily on the estimated module norms as the main output of the analysis, rather than the top-layer sources $\mathbf{s}$' which the multilayer computation eventually produces, because we expected to associate EEG features with the activity of cortical modules.

(Figure 1 is inserted around here)

2.2 Experiment procedures

2.2.1 Participants

A flow of this experimental procedure was illustrated in Figure 2. All participants were recruited by screening questionnaires and clinician assessment (n = 102: 49 females, 53 males; 29.88 ± 9.8 years old). Before the EEG-fMRI experiment, participants who had (i) inclination of suicidal thoughts measured in the BDI, (ii) currently/in the past mental/psychiatric diseases, (iii) did not understand the Japanese language. All received cash remuneration for their involvement after the experiment. Twenty-eight participants without psychiatric disease in the past could proceed to the EEG-fMRI experiment for two days. We excluded participants who had excessive body/head movements in the scanning of fMRI. Finally, seventeen participants completed the NF training experiment for four days. All participants provided written informed consent before the experiment. This study was approved by the ethics committee of the Advanced Telecommunications Research Institute International (ATR) and followed the Declaration of Helsinki.

(Figure 2 is inserted around here)

2.2.2 Psychological questionnaires

In the Screening experiment, all participants were conducted self-report questionnaires: the Beck Depression Inventory II (BDI-II), Rumination Response Scale (RRS), Obsessive-Compulsive Inventory (OCI), Autism-Spectrum Quotient (AQ), State-Trait Anxiety Inventory (STAI2), Snaith-Hamilton Pleasure Scale (SHAPS), Schizotypal Personality Questionnaire (SPQ), Barratt Impulsiveness Scale 11 (BIS-11), Zimbardo Time Perspective Inventory (ZTPI), and were rated on the 21-item Hamilton Depression

Rating Scale (HAM-D), the Hamilton Anxiety Rating Scale (HAM-A), and Structured Clinical Interview for DSM-IV-TR Axis disorders (SCID). To evaluate the effects of the EEG-based NF training, participants completed BDI-II, RRS, OCI, AQ, STAI2, BIS-11, and ZTPI on Day 1 (Visit 4) and Day 4 (Visit 7) in the NF training experiment.

2.2.3 N-back task

Participants had been conducted behavioral experiments, such as N-back tasks outside the MRI scanner: at the screening (Visit 1) to check baseline; at the NF training experiment (Day 1, Day 4) to examine the changes in cognitive performance due to the NF training. A homemade code using Presentation ® software (Version 18.0, Neurobehavioral Systems, Inc., Berkeley, CA) controlled the N-back task and displayed it on the monitor. When being ready to start the N-back task, participants had clicked a left bottom of a mouse at the beginning of each session. The participants had been instructed to be relaxed and simply focus on the center of the monitor. A single session consisted of four blocks with four conditions (0-back, 1-back, 2-back, 3-back) randomly aligned. A single trial had an inter-trial interval with 1300 ms duration and then displayed a number from 0 to 9 with 200 ms duration at the monitor center. In the 0-back condition, participants were asked to click the left button when appearing “0” on the monitor promptly. In the 1-back, 2-back, and 3-back conditions, participants were asked to promptly click the left button when matching a currently displayed number and a number presented one, two, or three trials beforehand. In total, a single block has consisted of 64 trials. Participants completed two sessions of the N-back task about 13 min.

In the EEG-fMRI experiment, participants also conducted the N-back task with EEG

recording outside of the MRI scanner and insight of the MRI scanner with fMRI scanning. In the MRI scanner, participants were asked to press the response buttons using MRI compatible response device (HHSC-2 × 2, Current Designs, Inc., PA, USA). A single session consisted of the first 30-s resting (a white fixation cross at the center of the screen), three blocks of three conditions (0-back, 1-back, and 2-back) with random order, the second 30-s resting, three blocks of the N-back tasks (0-back, 1-back, and 2-back) with random order, and the third 30-s resting. At the beginning of each block, participants saw a rule corresponding to the condition and then completed 20 trials.

2.3 Data acquisitions

MRI data were acquired with a 3T MRI scanner, MAGNETOM Verio (Siemens, Erlangen, Germany), using a Siemens 12-channel head coil installed in the Brain Activity Imaging Center in the ATR. High-resolution, T1-weighted structural images (TR = 2250 ms, TE = 3.06 ms, flip angle = 9 deg, inversion time = 900 ms, matrix = 256 x 256, 208 sagittal slices, 1 mm isotropic) were acquired for normalization to a standard brain for echo-planar image (EPI) registration purpose. Functional images such as fMRI data were acquired with an EPI sequence (TR = 2450 ms, TE = 30 ms, flip angle = 80 deg, matrix = 64 × 64, a field of view = 192 mm, slice thickness = 3.2 mm, 35 axial slices, scan sequence: ascending). We measured 150 volumes (6 min 7 s) for the resting state and 141 volumes (5 min 45 s) for the N-back task.

EEG data were measured with an MR-compatible amplifier (BrainAMP MR plus, Brain Products GmbH, Germany) and a 64-channel EEG electrode cap (BrainCap MR, Brain Products GmbH, Germany), providing 63 EEG channels and one electrocardiogram

(ECG) channel. According to the modified International 10-10 system, the EEG cap was placed corresponding to the EEG electrodes. The ground electrode and online reference electrode were placed on AFz and at FCz, respectively. For safety reasons, the impedances of all EEG electrodes and the ECG electrode were maintained lower than 10 kΩ and 50 kΩ, respectively, throughout the experiment. We placed the ECG electrode on the participant's back to obtain the electrocardiographic data to subsequently correct ballistocardiographic artifacts. A raw recording data was measured with 5 kHz sampling frequency filtering between 0.1 and 250 Hz using the Brain Vision Recorder (Brain Products GmbH, Germany). The amplifier system was placed beside the subject's head within the scanner during fMRI scanning with fixation of MR compatible sand backs to reduce artifact caused by tinny vibration of the MRI scanner. The EEG recording system clock was synchronized with a device (SyncBox, Brain Products GmbH, Germany) and the MRI scanner's 10 MHz master synthesizer to achieve phase synchronization clocks for digital sampling between the MRI data and the EEG system. For the artifact removal of the EEG data caused by the fMRI scanning, we simultaneously recorded each TR trigger signal to mark the onset time of every single fMRI volume acquisition. We used a projector (DLA-X7-B, JVC; frame rate = 60 Hz) to present the visual stimuli on an opaque screen in the EEG-fMRI data acquisition.

At the EEG-fMRI experiment, first, each participant completed EEG measurement of the resting-state (two sessions) and the N-back task (0-, 1-, 2-back; two sessions) in the soundproof shield room. A single session of the resting-state EEG and the N-back task took five minutes and six minutes, respectively. Second, participants moved to the MRI scanner and completed the resting-state (two sessions), the N-back task (two sessions),

the T1-weighted structural image scan, and the resting state (two sessions). Finally, EEG data (the resting-state: four sessions; the N-back task: four sessions) and EEG-fMRI data (the resting-state: eight sessions; the N-back task: four sessions) were taken to estimate the SPLICE filter for the neurofeedback.

At the NF training experiment, EEG signals were measured in the soundproof shield room from Day 1 to Day 3, then EEG-fMRI data were measured in the MRI scanner at Day 4 as well as the EEG-fMRI experiment. In the NF training (Day 1, 2, and 3), the resting-state EEG signals were measured for five minutes. Afterward, each participant conducted the NF training for 9 min in a single session, finally completed five sessions.

(Table1 is inserted around here)

2.4 Data analysis

2.4.1 Preprocess of fMRI

Figure 3 summarizes a flow of preprocessing of EEG and fMRI data and its integration process. We followed preprocessing parameters and methods from a previous study (Ogawa et al., 2018; Aihara et al., 2020). The data were processed using SPM8 (Wellcome Trust Centre for Neuroimaging). The first four volumes were removed to allow for T1 equilibration. The remaining data were applied slice-timing correction and realignment of the mean image of that sequence to compensate for head motion. The structural image was coregistered to the mean functional image and segmented into three tissue classes in the MNI space. The functional images were normalized and resampled single voxel size with a 2 × 2 × 2 mm grid. Finally, the normalized images

were spatially smoothed using an isotropic Gaussian kernel of 8 mm full-width at half maximum.

For each participant, we averaged fMRI time courses across all voxels within for each ROI. Linear regression was applied to remove mechanical, physiological, and other sources of spurious variance along with their temporal derivatives, including six motion parameters in addition to averaged signals over gray matter, white matter, and cerebrospinal fluid. Furthermore, to reduce spurious changes caused by head motion, the data were checked by a method that reduces motion-related artifacts. A high-pass filter (< 0.008Hz) was applied to these sets of time courses before the following regression procedure.

(Figure 3 is inserted around here)

2.4.2 EEG-fMRI integration analysis for selection of a module for NF training

For extraction of EEG network features, the SPLICE model was optimized from the resting-state EEG data simultaneously recorded with fMRI with leave-one-session out cross-validation for each individual. Before the training of the SPLICE model, the raw EEG data were cleaned as follows: remove the fMRI scanning and ballistocardiographic artifacts using Brain Analyzer (Brain Products); apply a bandpass filter between 8 and 12 Hz such as alpha band by EEGLAB (Delorme and Makeig, 2004). We decided to reduce 63, 20, and 20 dimensions for the first layer (sources), the second layer (modules), and the third layer (top-level ICs), respectively. We estimated EEG network features during the N-back task through the SPLICE model and then downsampled them at 5 Hz.

The EEG network features were convoluted with the hemodynamic response function (HRF) and decimated to match the time instant of the fMRI signal. We applied the general linear model for statistical evaluation with correlation analysis of fMRI signal (GLM, SPM12). The design matrix consisted of EEG network features, such as the output of twenty modules to identify whether a statistical cluster has existed in the DLPFC/MFC or PCC/Precuneus thresholding p-value < 0.001, uncorrected and cluster level $p < 0.05$ corrected by Family-Wised Error (FWE). Five participants whose a cluster was found in the DLPFC/MFC performed to upregulate the EEG network features, and three participants whose a cluster was identified in the PCC/precuneus performed to downregulate the EEG network feature in the NF training. Of course, the participants did not know which group they belong to and upregulation/downregulation until the end of the NF training.

2.5 Neurofeedback protocol

A real-time neurofeedback system consisted of software, OpenViBE (v1.0.0; Renard et al., 2010) for the real-time EEG signal acquisition, feedback module programmed by MATLAB, and Brain Amp MR (Brain Products) with 63-ch EEG electrode cap. EEG raw signals were acquired at 500 Hz through Brain Amp MR and OpenViBE Acquisition Server. In the interactive GUI, OpenViBE Designer, the EEG data was applied a bandpass filter between 8 and 12 Hz and electrooculography artifact removal (e.g., blinking, eye movement) using online recursive ICA (ORICA; Hsu et al., 2016). Afterward, the signals were put into the MATLAB wrapper that predicted EEG network features by the optimized SPLICE model. According to a selected SPLICE module in advance, an L2-norm of the module was estimated as a targeting EEG network feature. It then

displayed a feedback score depending on a task design. In this process, an output of the selected modules was downsampled at 5 Hz.

In the NF training, we modified a training protocol in a previous study of FCNef (Taylor et al., 2021) for EEG-NF. All participants have conducted a 5-min resting-state EEG recording and five neurofeedback sessions. We collected twenty trials in every single session. A single trial consisted of “rest” for 6 s, “induction” for 10 s, and “feedback” for 4 s. Feedback was calculated as a score (-1 to 1) presented as a circle on a monitor (Figure 4). For the NF group, the score was a difference of the mean power of between “induction” and “rest” period in logarithm scale into -1 to 1 in eleven steps (resolution = 0.2; if the score was less than -1 or more than 1, a circle size was minimum or maximum). Instead, for the sham group, the NF system randomly generated the score between -1 to 1. Participants were asked to try increasing a disc size as feedback on each trial by doing their best “do something with their brain” during the “induction” period. In the instructions, participants have been provided examples of strategies, e.g., mental calculation, recalling words, to help to imagine how to manipulate their own brain signals at the beginning of the training. Participants did not receive specific, explicit strategy associated with the analysis of feedback scores during the NF training; therefore, they tried to get larger feedback in trial by trial with own strategies.

After randomly dividing participants into two training groups (NF and sham), we applied two-sample t-test in Table2. We found no significant differences of depressive symptoms (BDI-II: $p = 0.257$; RRS: $p = 0.317$; AQ: $p = 0.815$; OCI: $p = 0.264$; STAI2(trait): $p = 0.512$).

(Table 2 and Figure 4 are inserted around here)

3. Results

3.1 Training effects on scores of psychological questionnaires

Table 3 summarizes the average (and standard deviation) scores on the questionnaires across two groups. Comparing the NF and sham groups, we calculated the effect sizes (Cohen's d) to evaluate the differences between post- and pre-NF for BDI-II and RRS with small samples. About the scores associated with depressive symptoms, we found large effect sizes in RRS (total: -0.722, brooding: -0.626, reflection: -1.050) but did not find large effect sizes in the BDI-II (total: 0.184). In other scores not directly related to depressive symptoms, we also found large effect sizes in AQ (total, attention switching), OCI (total, obsessing) in Supplemental Table1. The NF group showed another effect, an increase of STAI2 (trait) compared to the sham group but not in the STAI2 (state). Our results suggest that our NF training may reduce rumination, particularly subscales such as "brooding" and "reflection."

(Table3 is inserted around here)

3.2 The cognitive impact on neural representation due to the NF training

We evaluated changes of neural representation utilizing the NF training in a comparison of tasked fMRI data (N-back task) recorded on Visit 2 & 3 and Visit 7 (Day4). We did not collect the EEG-fMRI data on Visit 4 (Day1) because of practical reasons (scheduling of experiment and less burden on participants); therefore, we compared the fMRI data measured at Visit 2 & 3 as pre-NF training and Visit 7 as post-NF training in the GLM

analysis. To evaluate the interactions of groups (NF, sham) and time (Visit 2&3, Visit 7), we applied a full factorial design analysis for fMRI data during the N-back task using SPM12. We found two clusters with a contrast of 2-back > 0-back at the right angular gyrus and superior frontal gyrus 2 labeled by AAL toolbox thresholding by p-value < 0.001, uncorrected, and cluster-level p < 0.05 corrected by Family-Wised Error (FWE), cluster size > 244 voxels in Figure 5 and Table 4. About the behavioral performance of the N-back task during the EEG-fMRI simultaneous recording, we did not find significant effects observed in D-prime (D': signal detection analysis) or hit rates due to the NF training because of the ceiling effect (Table 5). It suggested that the neural basis of high cognitive load (2-back) could be processed with small efforts in these regions due to the NF training.

(Table 4, Table 5, and Figure 5 are inserted around here)

3.3 Changes of EEG-NF performance in the NF training

Participants in the NF group were given feedback scores calculated by the online EEG NF system on each trial end; therefore, we illustrated changes of the feedback scores across three days (Day1 to Day3, Figure 6). Four subjects showed an increased mean of the feedback scores at Day3 higher than the one at Day1, but other subjects did not show a training effect in the feedback score. From this result, we did not find a noticeable training effect represented in the feedback score.

(Figure 6 is inserted around here)

4. Discussion

In this study, we have extended the SPLICE for EEG-NF training and investigated the possibilities of EEG-NF for targeting depressive symptoms, particularly rumination-related brain regions in subclinical participants. Utilizing SPLICE with the EEG-fMRI simultaneous data before the NF training, we extracted EEG network features correlated with fMRI signals in the DLPFC/MFG or in the PCC/precuneus where the previous biomarker studies suggested (Ichikawa et al., 2020; Yamashita et al., 2020). Finally, we found large effect sizes in RRS (total, brooding, and reflection) compared to NF and sham groups. We start to discuss extractions of EEG network features with SPLICE, effects of EEG NF for depression symptoms protocol, its related neural basis, and methodological limitations of this study.

4.1 Improvement of depressive symptoms by EEG NF training

We expected that functional regularization in DMN or ECN might reduce depressive symptoms, such as BDI and RRS. We found a large effect size on RRS (total, brooding, and reflection) comparing the NF and sham groups. According to the previous FCNef training, Taylor et al. (2021) have conducted a four-day experiment for sub-clinical participants, then showed a significant reduction of BDI and RRS (brooding). Before FCNef training, a targeting FC was identified from functional ROIs by the N-back task, in the left DLPFC/MFG and the left PCC/precuneus as a functional localizer. During the training, feedback scores of the targeting FC were precisely calculated in a real-time manner; therefore, participants may easily control the feedback scores. In other recent results of Tsuchiyagaito et al. (2021), the feasibility of FCNef targeting FC between the right temporoparietal junction and the left precuneus was shown large effect size in a

difference between the NF and sham groups at the post-NF training on state-rumination assessed by VAS. Our result was consistent with the FCNef study of Taylor et al. (2021) that showed improvement of depressive symptoms associated with rumination, particularly brooding. The brooding factor is precisely thought to be associated with depression and mistake concern (Treynor et al., 2003; Hasegawa 2013), which characterize a part of melancholic depression. The EEG network features estimated with SPLICE were not directly calculated from the target FC like FCNef (Yamada et al., 2017; Taylor et al., 2021). In our case, we individually selected the SPLICE module by utilizing correlation analysis with time courses between EEG network features and fMRI data. It may help predict the network activity associated with DMN or ECN from EEG data on real-time processing in the NF training and support normalizing the targeting brain region.

A benefit of our protocol is that the fMRI information selects the EEG network feature. It helped to achieve the EEG NF training without fMRI scanning in the NF training. Other advanced approaches are simultaneous real-time fMRI and EEG NF (Zotev et al., 2020; Cury et al., 2020). An NF protocol of Zotev et al. (2020) simultaneously displayed bars of fMRI signals in the left amygdala and frontal EEG asymmetry in the alpha band. It was required to upregulate these bars involved with positive autographical memory. They conducted their NF protocols for major depressive disorder (MDD) patients and demonstrated through proof-of-concept to reduce depressive symptoms, the profile of mood state (POMS), and STAI. This method can directly modulate the target regions precisely. However, the costs of these treatments are prohibitive, and people who have claustrophobia cannot be applied. Our approach of EEG NF training using SPLICE demonstrated a possibility of treatment for depressive symptoms with low cost and

applicable in the realistic environment if we can select an optimal SPLICE module (not required MRI equipment). The module selection is one of the limitations of our protocol; therefore, further study needs to develop a methodology to choose optimal modules without fMRI information.

4.2 Training effect represented in fMRI activation during N-back task

In a comparison between pre-and post-NF, we found an interaction of brain activity with a group (NF, sham) and time (pre, post) in the right angular gyrus and superior frontal gyrus with a contrast of 2-back > 0-back. These brain regions were part of ECN and activated more significant MDD patients than healthy individuals (Fitzgerald et al., 2008). Through the NF training, participants in the NF group regularized their own brain activity in the closed-loop process. Therefore, the right frontal and parietal regions' calculation cost may be decreased even though the same cognitive load. In contrast, participants in the sham group could not succeed in making efforts to get higher scores in the NF training and may be required to do something to increase the size of the green disc in the induction period.

About the behavioral performance of the N-back task (0, 1, 2-back) on Visit 2 & 3 and Day 4 in the EEG-fMRI recording, we expected that the NF training improved the cognitive function of the NF group. However, in 0, 1, 2-back conditions, we did not find apparent differences because of the ceiling effect. One of the reasons is that we did not record EEG-fMRI of the 3-back task in our protocol, and we could not accurately evaluate their performance of working memory with a higher load. For healthy participants, we designed short-duration numeral presentation in our N-back task paradigm, such as 200

ms, but this was too easy in the case of 1 and 2-back conditions to see the effects of the NF training. We need to improve our N-back task protocol for future studies to evaluate the work memory performance correctly.

4.3 Methodological limitation

In this study, subclinical healthy participants completed the NF training. In our results, the scores of depressive symptoms were lower than in previous patient studies (Wang et al., 2019; Young et al., 2017; Zotev et al., 2020). Some participants were low scores from the beginning of the NF (Day 1) and did not show enough improvement due to the NF training because of the floor effect. Taylor et al. (2021) and Tsuchiyagaito et al. (2021) have conducted the NF training with healthy participants and are comparable to our study. One of the difficulties in recruiting appropriate participants for this experiment; in fact, we recruited about a hundred participants as screening for subclinical participants with depressive symptoms. To this end, we completed the NF training for seventeen participants; however, it was not enough samples to show stable statistics like Wang et al. (2019). To improve the sensitivity of pre-screening, we should conduct questionnaires not only BDI but also Self-rating Depression Scale (SDS; Zung, 1965).

For depressive symptoms, the EEG NF protocol of Wang et al. (2019) has demonstrated a proof of concept for patients with comorbid MDD and anxiety symptoms, comparing three groups, frontal alpha asymmetry (ALAY group), high-beta downregulation training (Beta group), and control. Eighty-seven patients completed ten sessions of NF training, twice a week, for five weeks. To this end, ALAY and Beta group showed a reduction of BDI-II by about 10 points, and a decrease of Beck Anxiety Inventory (BAI) score about eight points. Both psychological questionnaires showed significant interaction comparing

to the control group. This intensive and long-term NF training may be enough to induce significant effects on depressive symptoms. In our protocol, NF training was set for three days, and healthy individuals were recruited. There is a problem of scheduling and long-term treatment to achieve this NF training for a practical reason. For example, a protocol of Taylor et al. (2021) is four-day training, and another protocol of Tsuchiyagaito et al. (2021) and Zotev et al. (2020) is just one-day training. In making an NF protocol, the balance of training intensity and efficacy is crucial in practice; therefore, we must design the NF experiment carefully in further study.

We proposed SPLICE that extends ISA assumed hierarchical network structure in the EEG data to extract EEG network features. SPLICE automatically pools several highly correlated components in the optimization process and estimates the time course of network features, including several components. However, each extracted component was not considered a network structure which already known. For instance, for integration analysis of EEG-fMRI data, HRF-convoluted frequency powers were calculated to match time instants between EEG and fMRI data, then were applied GLM to identified brain regions or networks (Mantini et al., 2007). Another approach combines EEG-microstate analysis, which divides four to six states based on the clustering algorithm, then identifies brain regions using correlation analysis (Brechet et al., 2019; Al Zoubi et al., 2020). These methods may achieve dimension reductions and simply describe the relationship between fMRI and EEG data. To quantify the accuracy of the SPLICE model, we have to evaluate several conditions of EEG-fMRI data for future studies.

In sum, we proposed a new flame work of EEG NF training focusing on EEG network features combining with fMRI information such as the DLPFC/MFC and PCC/precuneus, which was related to ECN and DMN, respectively. We have examined an extension of SPLICE for the EEG NF training for depressive symptoms in sub-clinical healthy individuals by utilizing EEG network features. In the three-day NF training, we found a reduction of depressive symptoms such as rumination with two groups, NF training, and sham. Our results showed a possibility of transferable NF training from fMRI to EEG.

References

Aihara, T., Shimokawa, T., Ogawa, T., Okada, Y., Ishikawa, A., Inoue et al. (2020). Resting-state functional connectivity estimated with hierarchical Bayesian diffuse optical tomography. Front. Neurosci, https://doi.org/10.3389/fnins.2020.00032.

Beck, A. T., Steer, R. A., Brown, G. K. (1996). Beck Depression Inventory-II (BDI-II) The Psychological Corporation, Harcourt Brace; Toronto.

Cheon, E. J., Koo, B. H., Choi, J. H. (2016). The Efficacy of Neurofeedback in Patients with Major Depressive Disorder: An Open Labeled Prospective Study. Appl Psychophysiol Biofeedback, 41 (1), 103-10.

Cury, C., Maurel, P., Gribonval, R., Barillot, C. (2020). A Sparse EEG-Informed fMRI model for hybrid EEG-fMRI neurofeedback prediction. Front Neurosci, 13. https://doi.org/10.3389/fnins.2019.01451.

Delorme, A., Makeig, S. (2004). EEGLAB: an open-source toolbox for analysis of single-trial EEG dynamics, J Neurosci Methods, 134, 9-21.

Drysdale, A.T., Grosenick, L., Downar, J., Dunlop, K., Mansouri, F., Meng, Y. et al. (2017). Resting-state connectivity biomarkers define neurophysiological subtypes of depression. Nat Med. 23, 28–38.

Fitzgerald, P. B., Srithiran, A., Benitez, J., Daskalakis, Z. Z., Oxley, T. J., Kulkarni, J. et al. (2008). An fMRI study of prefrontal brain activation during multiple tasks in patients with major depressive disorder. Hum Brain Mapp. 29 (4), 490–501.

Hasegawa, A. (2013). Translation and initial validation of the Japanese version of the Ruminative Responses Scale. Psychol. Rep. 112, 716-726.

Hirayama, J., Hyvärinen, A., Kawanabe, M. (2017). SPLICE: fully tractable hierarchical extension of ICA with pooling. PMLR, 70, 1491-1500.

Hsu, S. H., Mullen, T. R., Jung T. P. (2016). Real-Time Adaptive EEG source separation using online recursive independent component analysis. IEEE Trans on Neural Syst Rehabil Eng. 24(3), 309-19.

Hyvärinen, A. and Hoyer, P. O. (2000). Emergence of phase and shift invariant features by decomposition of natural images into independent feature subspaces. Neural Comput, 12(7), 1705–1720.

Ichikawa, N., Lisi, G., Yahata, N., Okada, G., Takamura, M., Hashimoto, R. et al. (2020). Primary functional brain connections associated with melancholic major depressive disorder and modulation by antidepressants. Sci Rep. 10:3542, doi: 10.1038/s41598-020-60527-z.

Mantini, D., Perrucci, M. G., Cugini, S., Ferretti, A., Romani, G. L., Del Gratta, C. (2007). Complete artifact removal for EEG recorded during continuous fMRI using independent component analysis. Neuroimage, 34 82), 598-607.

Misaki, M., Tsuchiyagaito, A., Al Zoubi, O., Paulus, M., Bodurka, J., Tulsa 1000 Investigators. (2020). Connectome-wide search for functional connectivity locus associated with pathological rumination as a target for real-time fMRI neurofeedback intervention, Neuroimage Clin., 26(102244).

Northoff, G. (2016). Spatiotemporal psychopathology I: no rest for the brain's resting state activity in depression? Spatiotemporal psychopathology of depressive symptoms. J Affect Disord. 190, 854–66.

Ogawa, T., Aihara, T., Shimokawa, T., Yamashita, O (2018). Large-scale brain network associated with creative insight: combined voxel-based morphometry and resting-state functional connectivity analyses. Sci. Rep. 8. doi: 10.1038/s41598-018-24981-0.

Renard, Y., Lotte, F., Gibert, G., Congedo, M., Maby, E., Delannoy, V. et al. (2010). OpenViBE: an open-source software platform to design, test and use brain-computer interfaces in real and virtual environments, Presence, 19(1), 35-53.

Spielberger, C.D. (1983). State-trait anxiety inventory for adults. Palo Alto, CA: Mind Garden.

Taylor, J. E., Yamada, T., Kawashima, T., Kobayashi, Y., Yoshihara, Y., Miyata, J. et al. (2021). Reduction of brooding and more general depressive symptoms after fMRI neurofeedback targeting a melancholic functional-connectivity biomarker. medRxiv, https://doi.org/10.1101/2021.01.21.20248810.

Treynor, W., Gonzalez, R., Nolen-Hoeksema, S. (2003). Rumination reconsidered: A psychometric analysis. Cognit Ther Res. 27, 248−259.

Tsuchiyagaito, A., Misaki, M., Al Zoubi, O., Tulsa 1000 Investigators, Paulus, M., Bodurka, J. (2021). Prevent breaking bad: A proof of concept study of rebalancing the brain's rumination circuit with real-time fMRI functional connectivity neurofeedback, Hum Brain Mapp., 42, 922-940.

Wang, S. Y., Lin, I. M., Fan, S. Y., Tsai, Y. C., Yen, C. F., Yeh, Y. C. et al. (2019). The effects of alpha asymmetry and high-beta down-training neurofeedback for patients with the major depressive disorder and anxiety symptoms. J Affect Disord 257, 287–96.

Yamashita, A., Sakai, Y., Yamada, T., Yahata, N., Kunimatsu, A., Okada, N. et al. (2020). Generalizable brain network markers of major depressive disorder across multiple imaging sites. PLoS Biol. 18(12), e3000966.

Yamashita, A., Sakai, Y., Yamada, T., Yahata, N, Kunimatsu, A., Okada, N. et al., (2021). Common brain networks between major depressive-disorder diagnosis and symptoms of depression that are Validated for Independent Cohorts. Front. Psychiatry, 10 June 2021, https://doi.org/10.3389/fpsyt.2021.667881

Yahata, N., Kasai, K., Kawato, M. Computational neuroscience approach to biomarkers and treatments for mental disorders. Psychiatry Clin Neurosci. 71, 215–237 (2017).

Yamada, T., Hashimoto, R., Yahata, N., Ichikawa, N., Yoshihara, Y., Okamoto, Y. et al. (2017) Resting-state functional connectivity-based biomarkers and functional MRI-based neurofeedback for psychiatric disorders: a challenge for developing theranostic biomarkers. Int. J. Neuropsychopharmacol. 20, 769-781.

Young K.D., Zotev, V., Phillips, R., Misaki, M., Yuan, H., Drevets, W. C. et al. (2014). Real-time FMRI neurofeedback training of amygdala activity in patients with major depressive disorder. PloS One, 9, e88785.

Young, K.D., Siegle, G., J., Zotev, V., Phillips, R., Misaki, M., Yuan, H. et al. (2017). Randomized clinical trial of real-time fMRI amygdala neurofeedback for major depressive disorder: effects on symptoms and autobiographical memory recall. Am. J. Psychiatry, 174, 748-755.

Young, K.D., Zotev, V., Phillips, R., Misaki, M., Drevets, W.C., Bodurka, J. (2018). Amygdala real-time functional magnetic resonance imaging neurofeedback for major depressive disorder: A review. Psychiatry Clin Neurosci. 72(7), 466–481.

Yu, S. H., Tseng, C. Y., Lin, W. L. (2020). A neurofeedback protocol for executive function to reduce depression and rumination: a controlled study. Clin Psychopharmacol Neurosci, 18 (3), 375-385.

Zotev, V., Phillips, R., Yuan, H., Misaki, M., Bodurka, J. (2014). Self-regulation of human brain activity using simultaneous real-time fMRI and EEG neurofeedback. Neuroimage, 85, 985–95.

Zotev, V., Yuan, H., Misaki, M., Phillips, R., Young, K. D., Feldner, M. T. et al. (2016). Correlation between amygdala BOLD activity and frontal EEG asymmetry during real-time fMRI neurofeedback Training in Patients with Depression. Neuroimage Clin, 11, 224–38.

Zotev, V., Mayeli, A., Misaki, M., Bodurka, J. (2020). Emotion self-regulation training in major depressive disorder using simultaneous real-time fMRI and EEG neurofeedback.

Neuroimage. Clin 27, 102331.

Zotev, V., Bodurka, J. (2021). Linking amygdala blood oxygenation-level-dependent (BOLD) activity and frontal EEG in depression. The Neuroscience of Depression, Academic Press, pp. 301-310.

Zung, W. W. K. (1965). A self-rating depression scale. Arch Gen Psychiatry, 12, 63-70. doi: 10.1001/archpsyc.1965.01720310065008.

Conflict of Interest

The authors declare that the research was conducted in the absence of any commercial or financial relationships that could be construed as a potential conflict of interest.

Author Contributions

Takeshi Ogawa and Hiroki Moriya designed this study. Takeshi Ogawa and Nobuo Hiroe performed data acquisition. Takeshi Ogawa and Jun-ichiro Hirayama analyzed the data. Takeshi Ogawa, Jun-ichiro Hirayama, and Motoaki Kawanabe discussed data analysis and results. Takeshi Ogawa and Jun-ichiro Hirayama wrote the original draft.

Funding

This study was supported by JSPS KAKENHI Grant Number JP17H06041, JP18H05395, JP18KK0284, JP21K12620, JP21K12055, JP21H03516, the ImPACT Program of the Council for Science, Technology and Innovation (Cabinet Office, Government of Japan), CREST, JST, the MIC/SCOPE/ #192107002.

Acknowledgments

We thank Yoko Matsumoto for her help in recruiting participants, scheduling, and conducting the experiment; Kana Inoue and Tachi Kaori for their help in screening participants in the Screening experiment; Mihoko Sato, Ayumi Yuki, and Yoshiko Itakura for their supporting preparation of the EEG-fMRI and NF training experiments; Takashi Yamada for discussion to design the neurofeedback experiment; the ATR Brain Activity Imaging Center (BAIC), Akikazu Nishikido and Ichiro Fujimoto for their technical support.

Data Availability Statement

The data that support the findings of this study are available from the corresponding author, Takeshi Ogawa, upon reasonable request.

Contribution to the Field Statement

Several studies have reported advanced treatments for depressive symptoms, such as real-time fMRI neurofeedback. The fMRI neurofeedback focusing on a regularization of functional connectivity (FC) between executive control network (ECN) and default mode network (DMN) has been achieved to support the reduction of depressive symptoms. However, it is difficult to install this system in practice because the cost is high, and no practical signal processing techniques have existed to extract FC-related features from EEG. In this regard, stacked pooling and linear components estimation (SPLICE), recently proposed as a multilayer extension of independent component analysis and related independent subspace analysis, can be a promising alternative. However, its

application to the resting-state EEG has never been investigated. This method may help to modulate the target FC in the EEG-based neurofeedback training.

This study developed a real-time EEG neurofeedback system for improving depressive symptoms by using an EEG network features estimated by SPLICE. Utilizing information of the fMRI biomarker, we examined our paradigm for upregulation of the dorsolateral prefrontal cortex (DLPFC)/middle frontal cortex or downregulation of precuneus/posterior cingulate cortex (PCC). Finally, we found a large effect size in the rumination response scale compared to neurofeedback and sham groups. We demonstrated a possibility of EEG neurofeedback for depressive symptoms using EEG network features in the subclinical trials.

Figure legends

Figure 1.

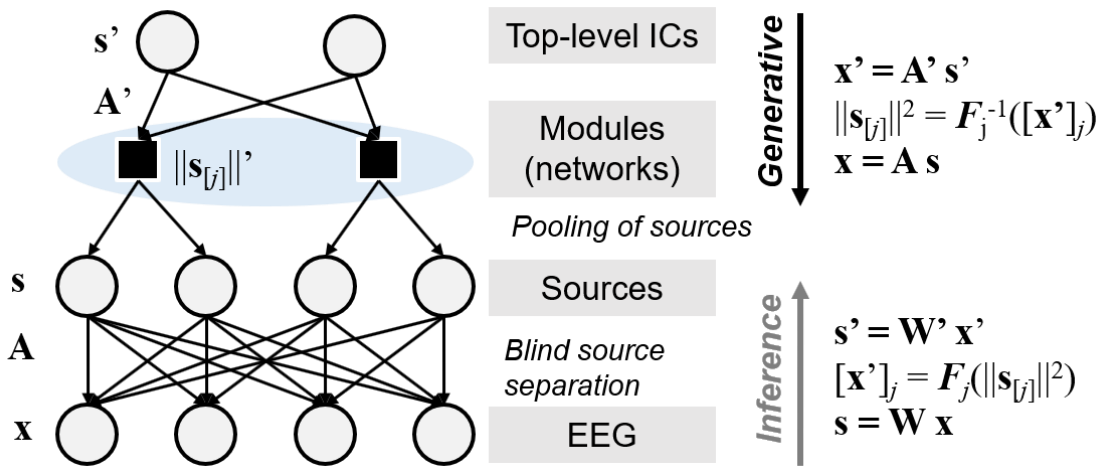

Figure1. Structure of SPLICE.

s: unobserved source signal; **A**: mixing matrix; **W**: demixing matrix of **A**; **x**: EEG measurements; **A**': invertible mixing matrix; **s**': source vector; F_j: link function; W': demixing matrix of **A**'.

Figure 2.

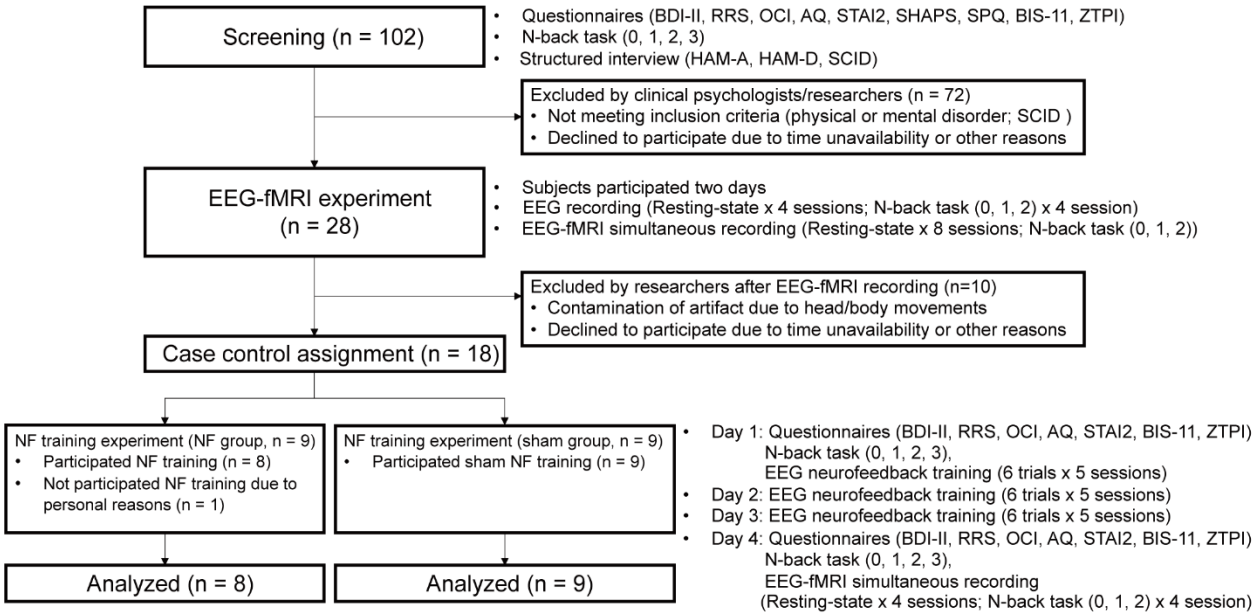

Figure2. A flow of the experiment

BDI-II: Beck Depression Inventory II; RRS: Rumination Response Scale; OCI: Obsessive-Compulsive Inventory; AQ: Autism-Spectrum Quotient; STAI2: State-Trait Anxiety Inventory, SHAPS: Snaith-Hamilton Pleasure Scale; SPQ: Schizotypal Personality Questionnaire; BIS-11: Barratt Impulsiveness Scale 11; ZTPI: Zimbardo Time Perspective Inventory; HAM-D: 21-item Hamilton Depression Rating Scale; HAM-A: Hamilton Anxiety Rating Scale; SCID: Structured Clinical Interview for DSM-IV-TR Axis disorders (SCID); NF: Neurofeedback.

762 **Figure 3.**

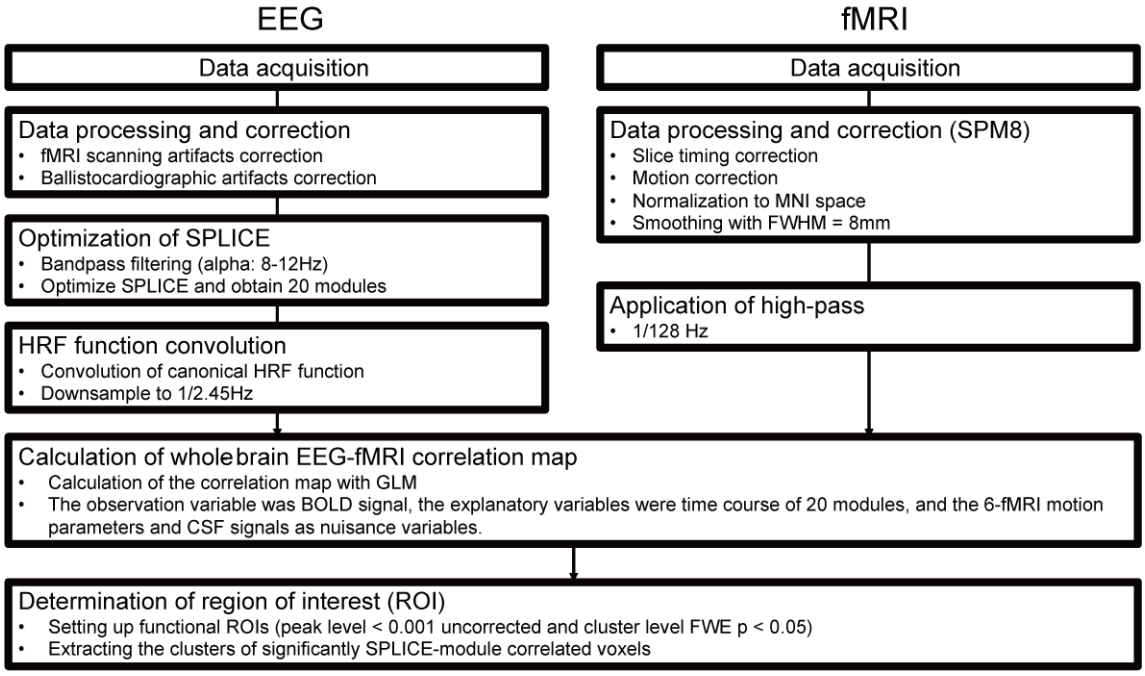

763

764 **Figure3. A flow of preprocessing of EEG-fMRI data and its integration analysis in**

765 **this study.**

766 SPLICE: stacked pooling and linear components estimation; HRF: hemodynamic

767 response function; MNI, Montreal Neurological Institute; FWHM, full width at half

768 maximum; GLM, General Linear Model; BOLD, blood-oxygen-level-dependent; CSF,

769 cerebrospinal fluid; FWE, family-wise error.

770

Figure 4.

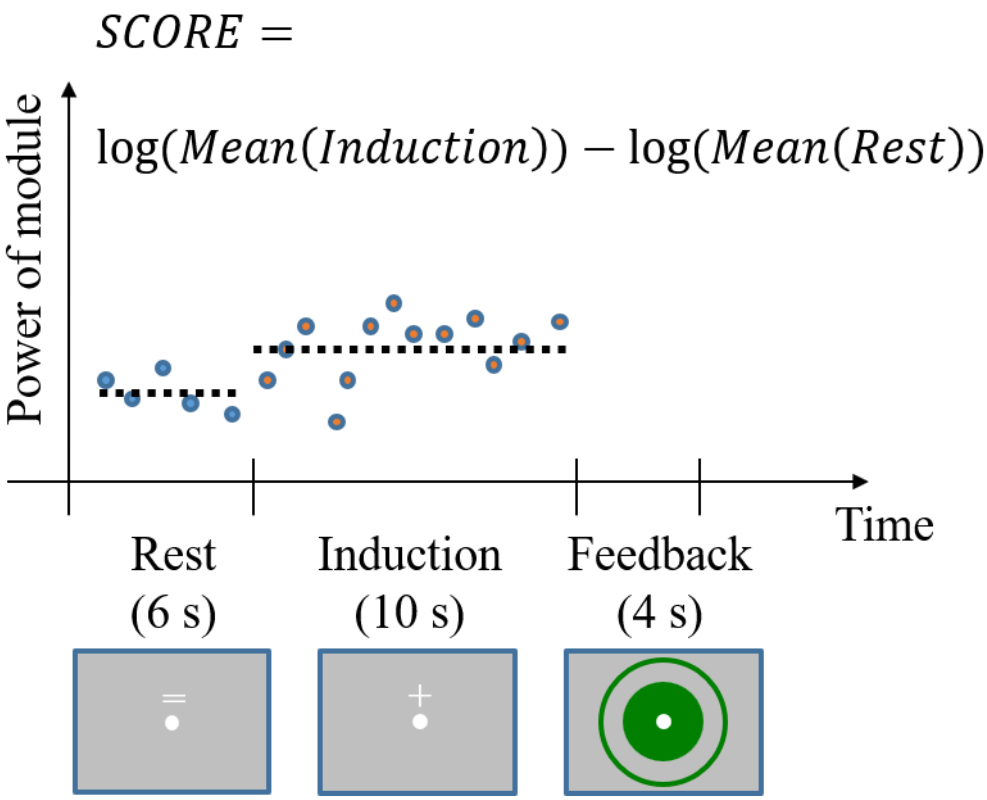

Figure4. A protocol of EEG NF training in a single trial.

Figure 5.

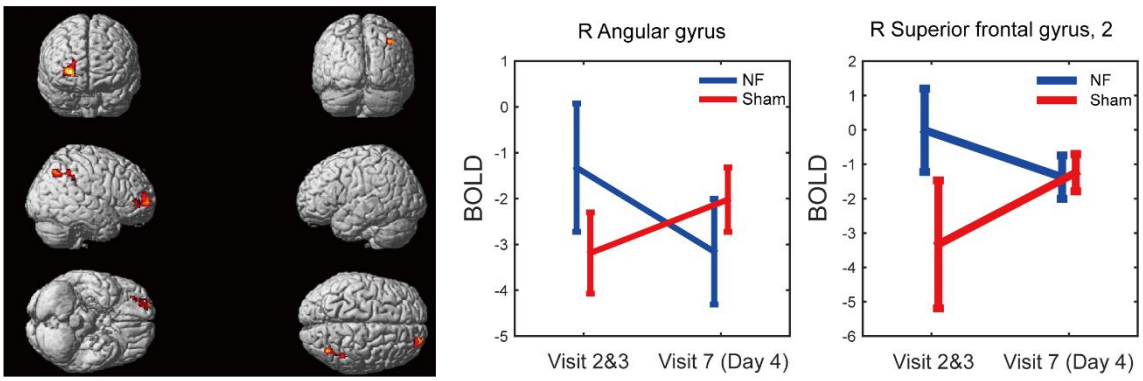

Figure 5. Identification of clusters illustrated the interaction of groups and times. Clusters showed significant interaction of group (NF, sham) and time (pre: Visit 2&3, post: Visit 7 (Day4)). A contrast was 2-back > 0-back, and labelled by AAL toolbox; thresholding by p-value < 0.001, uncorrected and cluster level p < 0.05 corrected by Family-Wised Error (FWE, cluster size > 244 voxels).

Figure 6.

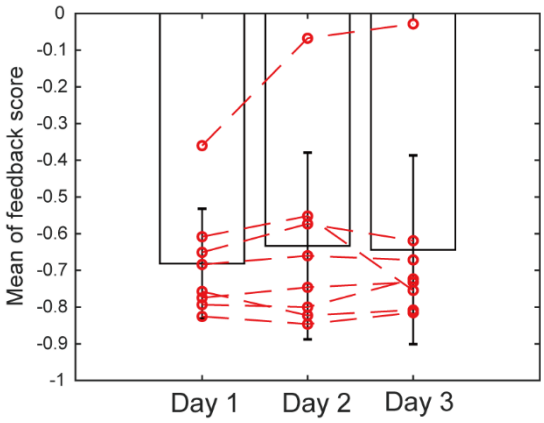

Figure 6. Changes of feedback scores across three-day NF training. The red dotted line showed the mean of feedback scores for each participant.

Tables

Table 1. Experimental Outline

	Screening	**EEG-fMRI**		**NF training**			
	Visit 1	Visit 2	Visit 3	Visit 4 (Day 1)	Visit 5 (Day 2)	Visit 6 (Day 3)	Visit 7 (Day 4)
Questionnaires	BDI-II, RRS, OCI, AQ, STAI2, SHAPS, SPQ, BIS_11, ZTPI	–	–	**BDI-II, RRS**, OCI, AQ, STAI2, BIS-11, ZTPI	–	–	**BDI-II, RRS,** OCI, AQ, STAI2, BIS-11, ZTPI
Structured interview	HAM-A, HAM-D, SCID	–	–	–	–	–	–
N-back task	0, 1, 2, 3	–	–	0, 1, 2, 3	–	–	0, 1, 2, 3
EEG data	–	-5-min resting state×4 -N-back task × 4 (0, 1, 2)		-5-min resting-state -NF training ×5	-5-min resting-state -NF training× 5	-5-min resting-state -NF training ×5	–

EEG-fMRI data	–	-5-min resting state×8 -N-back task×4 (0, 1, 2) -T1-weighted image	–	–	–	5-min resting state×4 -N-back task×2 (0, 1, 2) -T1-weighted image

NOTE: BDI-II: Beck Depression Inventory II; RRS: Rumination Response Scale; OCI: Obsessive-Compulsive Inventory; AQ: Autism-Spectrum Quotient; STAI2: State-Trait Anxiety Inventory, SHAPS: Snaith-Hamilton Pleasure Scale; SPQ: Schizotypal Personality Questionnaire; BIS-11: Barratt Impulsiveness Scale 11; ZTPI: Zimbardo Time Perspective Inventory; HAM-D: 21-item Hamilton Depression Rating Scale; HAM-A: Hamilton Anxiety Rating Scale; SCID: Structured Clinical Interview for DSM-IV-TR Axis disorders (SCID); NF: neurofeedback.

Table 2. The demographics of participants in the NF training

NOTE: NF: neurofeedback; BDI-II: Beck Depression Inventory II; RRS: Rumination Response Scale

Variables		**NF group (n = 9)**	**Sham group (n = 9)**	**p-value of t-test**
Age (years)		28.62 ± 10.84	25.97 ± 7.22	0.606
Gender	Female	2	2	
	Male	7	7	
BDI-II		7.89 ± 3.26	10.44 ± 6.50	0.257
RRS		40.67 ± 9.18	35.44 ± 12.91	0.317

Table 3. Comparison of statistical effect size associated with depressive symptom scores between NF and sham group

Variables	**NF group (n = 8)**		**Sham group (n = 9)**		**Cohen's d**
	Pre	**Post**	**Pre**	**Post**	
BDI-II (total)	5.25 (5.52)	3.75 (4.43)	7.22 (7.72)	5.33 (6.34)	0.184
-Cognitive depression	2.25 (3.37)	1.75 (2.76)	2.56 (3.47)	2.44 (3.05)	-0.390

-Somatic depression	3.00 (3.46)	2.00 (2.61)	4.67 (4.66)	2.89 (3.76)	0.479
RRS (total)	31.00 (5.68)	28.25 (4.40)	31.33 (8.00)	31.67 (8.70)	-0.722
-Brooding	7.50 (5.68)	6.63 (1.92)	7.78 (2.11)	7.89 (2.93)	-0.626
-Depression	16.25 (2.96)	15.88 (2.95)	17.67 (5.48)	17.56 (5.00)	-0.101
-Reflection	7.25 (1.98)	5.75 (0.89)	5.89 (1.45)	6.22 (1.64)	-1.050

Table 4. Comparisons of Pre (Visit 2 & 3)/Post (Day 4) fMRI data during N-back task.

Brain region	Peak coordinate (MNI)			Cluster size		Details
	X	Y	Z	Voxels	The peak of T score	
0-back task						
R Angular gyrus	38	-66	44	244	5.38	R Angular R Inferior parietal gyrus R Supramarginal gyrus
R Superior frontal gyrus, 2	34	44	2	330	4.17	R Superior frontal gyrus, 2 R Middle frontal gyrus, 2

Table 5. Comparison of N-back task performance during EEG-fMRI simultaneous recording

		NF group		Sham group		Cohen's d
Measure	Level	Visit 2 & 3 (pre)	Visit 7 (post)	Visit 2 & 3 (pre)	Visit 7 (post)	
D'	0-back	4.12 ± 0.1	4.32 ± 0.1	4.32 ± 0.1	4.28 ± 0.1	0.48
	1-back	3.85 ± 0.6	4.11 ± 0.4	4.20 ± 0.4	4.28 ± 0.2	0.33
	2-back	3.18 ± 0.9	3.67 ± 0.7	3.52 ± 0.7	3.81 ± 0.6	0.30
p (hit)	0-back	0.93 ± 0.2	0.99 ± 0.0	0.99 ± 0.0	0.99 ± 0.0	0.50
	1-back	0.90 ± 0.2	0.96 ± 0.1	0.98 ± 0.1	0.99 ± 0.0	0.36
	2-back	0.81 ± 0.2	0.91 ± 0.1	0.88 ± 0.1	0.94 ± 0.1	0.22